

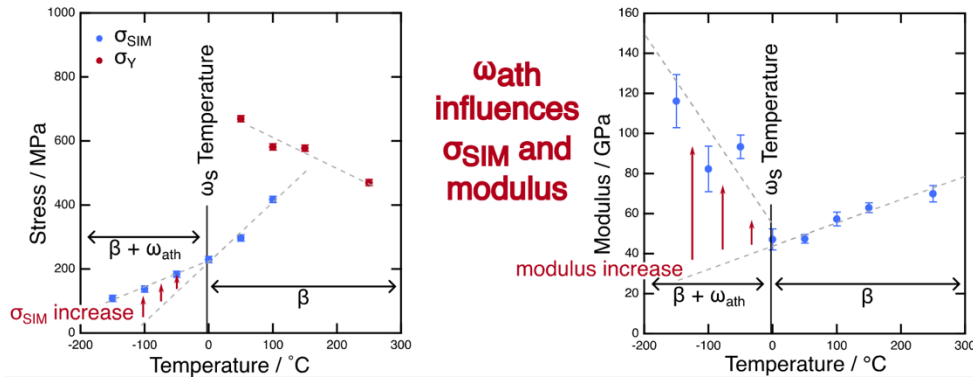
The effect of athermal omega on the transformation behaviour of Ti-24Nb-4Zr-8Sn (wt%)

N.L Church¹, J.Y. Ang¹, O.G. Reed¹, O.E. Gibson¹, N.G Jones^{1*}

¹ Department of Materials Science and Metallurgy, 27 Charles Babbage Road, Cambridge, CB3 0FS, University of Cambridge, UK

* Corresponding author email: ngj22@cam.ac.uk

Graphical Abstract



Abstract

Ti-Nb based alloys are candidate materials for orthopaedic and orthodontic applications due to a low elastic modulus and superelastic properties. However, many of these alloys are also susceptible to a transformation to the hexagonal ω phase. When ω is formed isothermally it can stiffen and embrittle the alloy, however, there is a limited understanding of the role it plays when formed athermally on cooling, with many conflicting statements made within the literature. As such, this study assesses the role of athermally formed ω on the superelastic behaviour and elastic modulus of the exemplar superelastic alloy, Ti-24Nb-4Zr-8Sn. It was found that the ω phase raised the modulus and the stress required for superelastic behaviour. This highlights the need to design alloys resistant to both forms of the ω phase, for low modulus superelastic alloys to be produced.

Metastable β Ti alloys have received considerable attention for use as orthopaedic and orthodontic implant materials due to their excellent biocompatibility, intrinsic corrosion resistance, low elastic modulus and an ability to display superelastic properties [1–3]. The superelastic transformation from the bcc β phase to the orthorhombic α'' martensite relies on suppressing the formation of the thermodynamically stable hcp α phase. This results in a β phase that is metastable at the testing temperature such that the alloy is susceptible to the shear transformation to the α'' martensite [4,5]. However, this metastability means these materials are also vulnerable to the formation of the hexagonal ω phase, which can increase the material stiffness and influence the transformation behaviour [6,7].

The ω phase can exist in one of two forms, which are crystallographically identical but compositionally distinct, and can be distinguished based on their formation mechanism [8]. Isothermal ω (ω_{iso}) typically forms at intermediate temperatures between ~ 100 – 500°C depending on the alloy composition [9]. This form of ω relies on atomic rearrangement and results in a Ti rich precipitate within the β matrix [10]. It is commonly reported that ω_{iso} is highly detrimental to mechanical behaviour, embrittling and stiffening the alloy [6,10,11], and preventing a transformation to α'' [12].

The other form of the ω phase, athermal ω (ω_{ath}), forms without diffusion on cooling from elevated temperatures. This can occur by one of two mechanisms; either via the “frozen phonon” mechanism when cooling rapidly from the β phase field [13], or when cooling below a well-defined temperature, the ω start temperature (ω_s) [14]. ω_{ath} is therefore present in many metastable β Ti alloys following solution heat treatment.

Despite its prevalence, the effect of ω_{ath} on the mechanical behaviour of metastable β Ti alloys is poorly understood. Studies comparing the role of ω_{ath} and ω_{iso} have highlighted significant differences between their effect on mechanical behaviour [15]. However, within the literature this distinction is sometimes unclear, with the negative implications of the two types often considered to be equal in magnitude. Possibly because of this,

41 many design criteria for low modulus structures highlight the importance of suppressing the ω_{ath} phase on
42 cooling to achieve low stiffnesses [16,17] and better match the mechanical properties of bone. Furthermore,
43 some of the lowest modulus alloys that have been produced contain elements such as Sn, which are thought
44 to aid in the suppression of the ω phase [16,18,19]. Despite this, other studies have suggested that ω_{ath} has
45 only a limited effect on the alloy stiffness [6].

46 The effect of ω_{ath} on the superelastic transformation to α'' is equally unclear. Some studies report that ω_{ath}
47 competes with α'' on cooling with one forming to the exclusion of the other [9,20]. ω_{ath} has also been suggested
48 to suppress the martensitic transformation during subsequent mechanical deformation [21]. In contrast, other
49 reports suggest that ω_{ath} does not prevent a β to α'' transformation and instead α'' can consume the ω_{ath} phase
50 as the α'' lath extends into the β grain [22,23]. Furthermore, studies on alloys containing ω_{ath} have
51 demonstrated that both thermally and mechanically induced martensitic transformations are possible [14,24–
52 26], and both α'' and ω_{ath} can form concomitantly on cooling [27].

53 However, the extent to which ω_{ath} may influence the β to α'' transformation remains unclear. For example,
54 whilst it has been suggested that ω_{ath} does not prevent α'' formation, its presence may still influence the stress
55 or temperature at which α'' can form [28]. In that study, the critical stress required to exhibit non-linear
56 behaviour (σ_{SIM}) was measured and seen to decrease linearly as a function of temperature, consistent with
57 the Clausius-Clapeyron relationship [29,30]:

$$58 \quad \frac{d\sigma_{\text{SIM}}}{dT} = \frac{dS}{d\varepsilon} \rho$$

59 Where $d\sigma_{\text{SIM}}$ is the change in transformation stress with a change in temperature, dT . dS is the entropy change
60 between the β and martensite structures, ρ is the density of the alloy and $d\varepsilon$ is the transformation strain
61 between β and α'' .

62 However, below a certain temperature, the trend changed and the stress required to transform to α''
63 increased. However, the presence of ω was assessed via laboratory-based diffraction techniques where the
64 detection of ω necessitates its presence in larger volume fractions than may be expected in many Ti-Nb based
65 alloys. Furthermore, other mechanisms such as detwinning of α'' would also be expected to result in an, albeit
66 small, increase in the stress required for non-linear behaviour as temperature is reduced, with many of the
67 compositions in the study reported to exhibit shape memory behaviour.

68 Despite this, studies on Ti-Nb based alloys with higher β phase stability also display similar trends in behaviour,
69 for example, in the Ti-Nb-Ta system [31]. The temperature at which the deviation from the Clausius-Clapeyron
70 relationship occurred was lower for alloys with a higher β phase stability. However, ω was reportedly present
71 in TEM diffraction patterns at temperatures greater than those at which this change in gradient was observed,
72 suggesting the cause of this response may be the result of a different underlying mechanism.

73 Other studies considering a systematic variation in alloy composition have also identified changes in the trend
74 of M_s temperature between alloys containing ω_{ath} , and those without ω_{ath} , similarly suggesting a deviation
75 from the Clausius-Clapeyron relationship [32,33]. However, the presence of ω was again identified via
76 laboratory-based techniques, necessitating larger volume fractions of ω . Furthermore, the variation in
77 composition would also be expected to influence other aspects of the transformation, and therefore similarly
78 be expected to influence the Clausius-Clapeyron relationship. Firstly, it may influence the heat treatment, and
79 generation of residual stresses on cooling, both of which have been shown to be important parameters
80 affecting the M_s temperature [24,34]. Secondly, a change in composition would influence the entropy of
81 transformation from the β to α'' phases, and has been shown in numerous studies to significantly influence
82 the transformation strain from β to α'' [35–37].

83 Understanding the role of ω_{ath} on the transformation behaviour is challenging as ω_{ath} in most superelastic
84 materials is typically a nanoscale phase present in relatively low volume fractions within the microstructure
85 [38,39]. This necessitates employing high energy diffraction techniques to study alloys containing the ω phase.
86 Such techniques have the resolution to detect even small volume fractions of ω_{ath} within a sample and can
87 facilitate an *in situ* assessment of the transformation behaviour [14,27,40].

88 This study therefore uses a combination of *in situ* and *ex situ* techniques to understand the effect of ω_{ath} on
89 the mechanical behaviour of an exemplar commercial Ti-Nb based alloy, Ti2448 (Ti-24Nb-4Zr-8Sn, wt%), with
90 a low susceptibility to the ω phase. This is achieved by investigating the mechanical response of the alloy across

91 a range of temperatures (from -150°C to 250°C), at some of which the ω_{ath} phase is present. Samples of a 2 mm
92 thick commercially supplied plate of Ti2448 were rolled to 0.5 mm final thickness. Flat rectilinear dog-bone
93 tensile samples with $\sim 0.5 \times 0.5 \text{ mm}^2$ gauge cross-section, and 14 mm gauge length were prepared by wire
94 electro discharge machining (EDM) and then sealed in evacuated quartz ampoules with Ta foil as a getter for
95 oxygen. Samples were then inserted into a pre-heated box furnace and solution heat treated at 900°C for 5
96 min. The furnace temperature was calibrated to $\pm 1 \text{ }^\circ\text{C}$ with the use of an N-type thermocouple. Samples were
97 subsequently quenched into ice water with the ampoule remaining intact.

98 *In situ* synchrotron X-ray diffraction (sXRD) data were acquired at the I12 beamline at Diamond Light Source in
99 transmission Debye-Scherrer geometry. The X-ray energy ($\sim 80 \text{ keV}$) was calibrated with a NIST CeO_2 standard
100 sample at multiple sample-to-detector distances. Diffraction data were acquired from tensile samples secured
101 in negative impression grips in a Linkam TST350 using a 1 s exposure and a Pilatus 2D CdTe detector. Samples
102 were heated or cooled within the test frame under an inert N_2 atmosphere at $25 \text{ }^\circ\text{C min}^{-1}$, and then loaded at a
103 cross-head displacement rate of $4 \text{ } \mu\text{m s}^{-1}$.

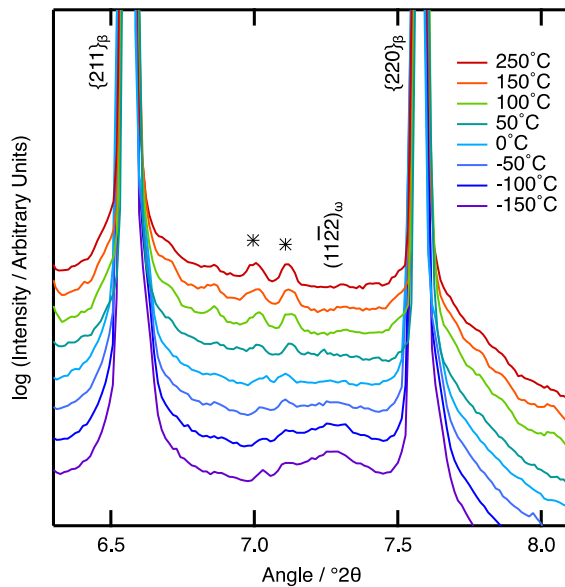
104 The ω_s temperature was determined by fitting a unique ω phase reflection with a gaussian in WaveMetrics
105 Igor Pro 9 and monitoring the peak area as a function of temperature. ω_s was then taken as the temperature
106 above which the ω phase reflection could no longer be discerned from the background. The critical stress
107 required to form α'' (σ_{SIM}) was determined from the *in situ* data by using the same methodology to fit an α''
108 peak and identifying the stress at which the peak became discernible from the baseline. The errors in σ_{SIM}
109 were determined by considering the stress resolution of the diffraction data.

110 *Ex situ* digital image correlation (DIC) data were acquired using the same test frame and testing parameters. A
111 $10 \text{ } \mu\text{m}$ speckle pattern was applied to the gauge of each specimen using an Iwata CM-B airbrush. Images were
112 acquired at a rate of 2 s^{-1} during deformation using an LaVision Imager E-lite camera, with an exposure time of
113 $1100 \text{ } \mu\text{s}$. These images were then analysed using DaVis software to obtain an average strain over the sample
114 for each frame.

115 The modulus of each sample was determined by fitting a linear function to the initial portion of the stress-
116 strain curve. *In situ* σ_{SIM} values were considered in each case, to ensure that the modulus was only measured
117 during the linear-elastic regime. σ_{SIM} and σ_Y were determined from the *ex situ* data by offsetting the linear fit
118 and considering an intersection of this line with the data. The linear offsets used were 0.05 % strain for σ_{SIM}
119 and 0.2 % for σ_Y , with the latter consistent with proof stress calculations in ASTM E8 [41]. Errors in these
120 measurements were obtained by considering the errors in the measurement of cross sectional area of each
121 sample. Separate linear trend lines were fit to the data above and below ω_s , by weighting each datapoint by
122 its associated error bar.

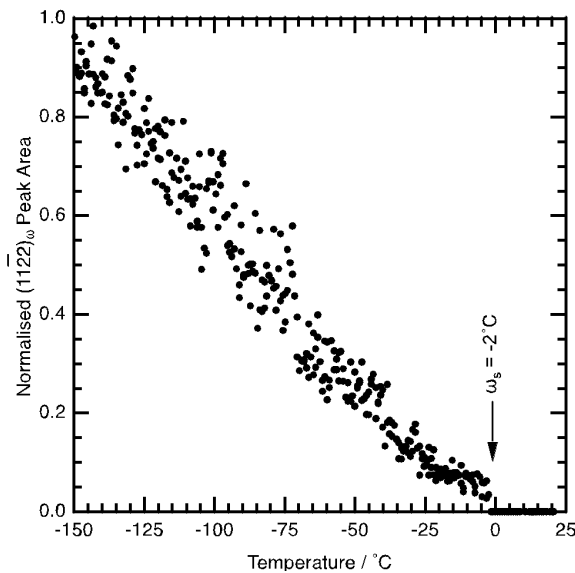
123 To assess the initial condition of each sample, sXRD patterns were acquired at the test temperature of each
124 sample, shown in Figure 1. At all temperatures, strong reflections consistent with the β phase were present.
125 At the lower test temperatures, a broad reflection consistent with the ω phase was also present. None of the

126 samples contained any evidence of the α'' martensite, suggesting the M_s temperature is below -150°C . The two
 127 peaks indicated by the asterisk, present in all patterns, are known artefacts relating to the EDM process.
 128



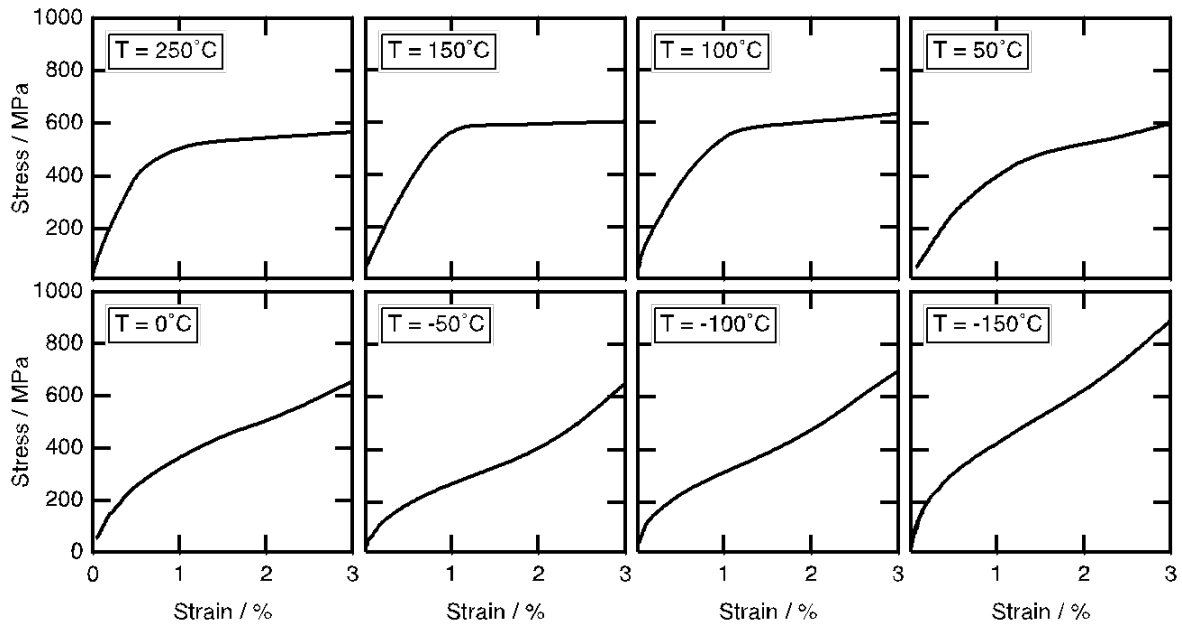
129 Figure 1. sXRD diffraction patterns highlighting the phases present at the test temperature of each sample.

130 To measure the ω_s temperature, the $(11\bar{2}2)_\omega$ reflection was monitored on cooling from 25 to -150°C and the
 131 peak area taken as a proxy to volume fraction. The ω peak intensity was normalised to the value at -150°C with
 132 these data given in Figure 2. The temperature at which the ω phase reflection could no longer be discerned
 133 from the baseline was taken as ω_s , at $\sim -2^\circ\text{C}$. This demonstrated that samples tested at 0°C and above contained
 134 solely the β phase, whereas samples tested at -50°C and below, comprised a $\beta + \omega_{\text{ath}}$ structure.



135
 136 Figure 2. Evolution of the $(11\bar{2}2)_\omega$ reflection on cooling the sample.

137 The mechanical behaviour at each testing temperature was evaluated *ex situ* using DIC, with the corresponding
 138 σ - ϵ data shown in Figure 3. These tests were repeated *in situ* to provide information regarding the deformation
 139 processes occurring within the material. At temperatures of 250°C and 150°C , the sample initially deformed in
 140 a linear-elastic manner. Above ~ 400 and 600 MPa respectively, there was a significant deviation from linear
 141 behaviour, and a large accumulation of strain. There was no evidence of any transformation to α'' within the
 142 diffraction data when tested at these temperatures, and hence, this deviation from linear behaviour
 143 corresponds to the onset of slip.



144

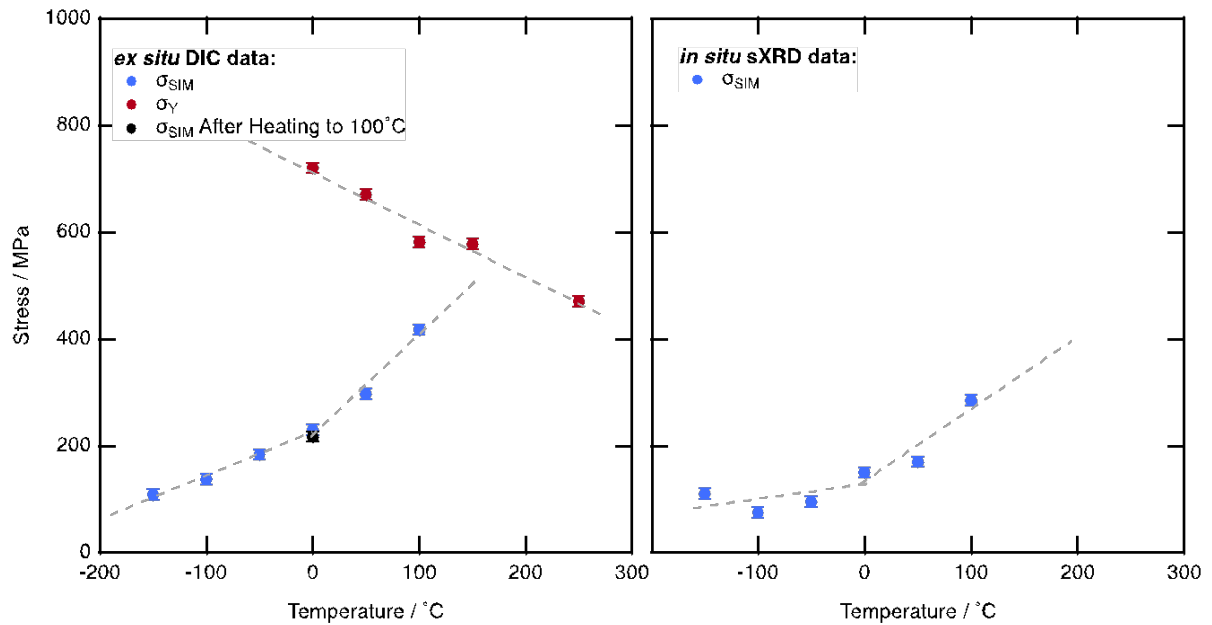
145 *Figure 3. Mechanical testing data of Ti2448 at different temperatures.*

146 At all other test temperatures, the samples initially deformed in a linear-elastic manner before some deviation
 147 from linear. This deviation coincided with the evolution of diffraction peaks corresponding to α'' , and hence is
 148 taken as σ_{SIM} . At higher stresses, there was a second decrease in gradient observed within the *ex situ* data
 149 consistent with slip.

150 The stresses at which these changes in gradient were observed are displayed graphically as a function of
 151 temperature in Figure 4. The σ_{SIM} values from the *in situ* data were determined to be the stresses at which the
 152 first α'' peak could be distinguished from the baseline. These data are also given in Figure 4.

153 The yield stress for the alloy was shown to decrease approximately linearly with an increase in test
 154 temperature, as expected. At test temperatures above ω_s , the value of σ_{SIM} increased linearly up to 100°C,
 155 consistent with the Clausius-Clapeyron relationship. At higher test temperatures of 150°C and 250°C, there was
 156 no evidence of any stress induced transformation to α'' , in either the *in situ* or *ex situ* data. Due to the decrease
 157 in yield stress, and increase in σ_{SIM} with temperature, this change in primary deformation mechanism can be
 158 readily understood. By extrapolating the gradient of σ_{SIM} to higher temperatures, the value of σ_{SIM} is estimated
 159 to exceed the yield stress at temperatures above $\sim 150^\circ\text{C}$. As such, the material will deform by conventional
 160 plastic flow above these temperatures with no formation of α'' .

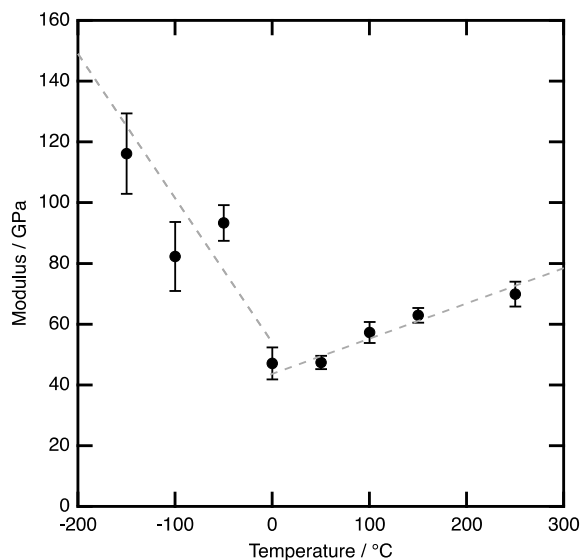
161 Interestingly, at temperatures below ω_s , the value of σ_{SIM} also varied linearly, however at a shallower gradient.
 162 Previous studies on this alloy have shown that heating samples to elevated temperatures has resulted in
 163 increased values of σ_{SIM} in subsequent room temperature mechanical tests [42]. Unfortunately, all samples
 164 tested above ω_s were heated to the test temperature, whereas all samples below ω_s were cooled to their test
 165 temperature. As such, it is unclear whether this change in gradient of σ_{SIM} is a result of the ω transformation,
 166 or a function of heating the samples to elevated temperatures. Hence, an additional sample was first heated
 167 to 100°C and then cooled and tested at 0°C. If ω_{ath} were directly responsible for the change in gradient of σ_{SIM} ,
 168 it would be expected that the value of σ_{SIM} obtained would be unchanged with respect to the sample cooled
 169 directly to 0°C. If, however, heating the sample was governing the change in response, it would be expected
 170 that the value of σ_{SIM} would be elevated compared to the sample directly cooled to 0°C. Here, the value of
 171 σ_{SIM} for this test is also shown alongside the other data in Figure 4. σ_{SIM} was shown to be the same (within
 172 error) of the value obtained without any prior heating step. This highlights that the change in gradient is related
 173 to the formation of ω_{ath} .



174
 175 *Figure 4. In situ and ex situ values of σ_{SIM} obtained at each test temperature. The ex situ data also contains measurements of the*
 176 *yield stress and the value of σ_{SIM} at 0°C following heating the sample to 100°C.*

177 By extrapolating the higher temperature gradient to temperatures where ω_{ath} is present, the effect of ω_{ath} can
 178 be readily rationalised. Hence, whilst ω_{ath} does not prevent the transformation to α'' , ω_{ath} is acting to increase
 179 the stress required to transform to α'' . The effect on transformation stress is significant given the very low
 180 volume fractions of ω_{ath} present in the sample.

181 The Young's modulus values of the sample at each test temperature are shown in Figure 5. There is a minimum
 182 in the modulus around ω_s . Above and below this value the modulus of the alloy increases. This increase is most
 183 dramatic for the test performed below ω_s , highlighting the significant stiffening effect caused by ω_{ath} as its
 184 volume fraction increases. It has been reported that the stiffening effect of ω_{ath} can be explained by the
 185 subsequent diffusion of oxygen into the phase [43], resulting in a precipitate that more resembles ω_{iso} .
 186 However, in the present study, the stiffness is greater at colder temperatures, where diffusion is significantly
 187 more limited. For elevated temperatures, the increase in modulus is not particularly pronounced, but may be
 188 related to an increase in stability of the parent β phase, and hence a lower susceptibility to shear
 189 transformations. Previously, an increase in β phase stability has been shown to result in an increase in the
 190 modulus, both for Ti2448 and other alloys [16,44].



191
 192 *Figure 5. Values of the modulus of each sample, tested at different temperatures.*

193 In summary, changes in mechanical behaviour of Ti2448 can be seen to directly correlate with the onset of ω_{ath}
194 in this alloy. This includes both a significant stiffening of the alloy and an increase in the stress required to form
195 α'' . Not only do these data rationalise some of the trends observed within the literature, but they also provide
196 the first unambiguous experimental evidence, elucidating the role of small volume fractions of ω_{ath} on the
197 mechanical response of Ti-Nb based alloys.

198 This observation has direct consequences for the development of new Ti-Nb biomedical alloys as it serves to
199 highlight the critical need to avoid ω_{ath} formation, both to achieve low modulus structures, and to facilitate
200 easy transformation to α'' .

201 Acknowledgments

202 The authors would like to thank Diamond Light Source for the provision of beamtime under MG33585. The
203 authors would also like to thank Dr Stefan Michalik for his assistance collecting the synchrotron diffraction
204 data.

205 Dataset DOI

206 The research data required to reproduce these findings are available from the University of Cambridge
207 repository.

208 DOI: 10.17863/CAM.111759

209 Credit

210 NL Church: Conceptualization; Methodology; Validation; Formal Analysis; Investigation; Writing – Original
211 Draft; Visualisation. J.Y. Ang: Formal Analysis; Investigation. O.G. Reed: Methodology; Formal Analysis;
212 Investigation. O.E. Gibson: Formal Analysis. NG Jones: Methodology; Investigation; Resources; Writing –
213 Review & Editing; Supervision; Project Administration; Funding Acquisition.

214 Conflict of Interest

215 The authors declare that they have no known competing financial interests or personal relationships that could
216 have appeared to influence the work reported in this paper.

217 References

- 218 [1] H.Y. Kim, S. Miyazaki, Ni-Free Ti-Based Shape Memory Alloys, Elsevier, 2018.
- 219 [2] P. Pesode, S. Barve, A review—metastable β titanium alloy for biomedical applications, Journal of
220 Engineering and Applied Science 70 (2023). <https://doi.org/10.1186/s44147-023-00196-7>.
- 221 [3] R.P. Kolli, A. Deveraj, A Review of Metastable Beta Titanium Alloys, Metals (Basel) 8 (2018) 1–41.
222 <https://doi.org/10.3390/met8070506>.
- 223 [4] C. Leyens, M. Peters, Titanium and Titanium Alloys, 2003.
- 224 [5] G. Lutjering, J. Williams, Titanium, 2007.
- 225 [6] J. Nejezchlebová, M. Janovská, H. Seiner, P. Sedlák, M. Landa, J. Šmilauerová, J. Stráský, P. Hrcuba, M.
226 Janeček, The effect of athermal and isothermal ω phase particles on elasticity of β -Ti single crystals,
227 Acta Mater 110 (2016) 185–191. <https://doi.org/10.1016/j.actamat.2016.03.033>.
- 228 [7] C.H. Wang, M. Liu, P.F. Hu, J.C. Peng, J.A. Wang, Z.M. Ren, G.H. Cao, The effects of α'' and ω phases on
229 the superelasticity and shape memory effect of binary Ti-Mo alloys, J Alloys Compd 720 (2017) 488–
230 496. <https://doi.org/10.1016/j.jallcom.2017.05.299>.
- 231 [8] S.M. Dubinskii, A. Korotitskiy, S. Prokoshkin, V. Brailovski, In situ X-ray diffraction study of athermal and
232 isothermal omega-phase crystal lattice in Ti-Nb-based shape memory alloys, Mater Lett 168 (2016)
233 155–157. <https://doi.org/10.1016/j.matlet.2016.01.012>.
- 234 [9] B.S. Hickman, The formation of omega phase in titanium and zirconium alloys: A review, J Mater Sci 4
235 (1969) 554–563. <https://doi.org/10.1007/BF00550217>.

- 236 [10] J.A. Ballor, T. Li, F. Prima, C.J. Boehlert, A. Devaraj, A review of the metastable omega phase in beta
237 titanium alloys: the phase transformation mechanisms and its effect on mechanical properties,
238 *International Materials Reviews* 68 (2022) 26–45. <https://doi.org/10.1080/09506608.2022.2036401>.
- 239 [11] A.X.Y. Guo, C. Geng, Z. Lin, S.C. Cao, A Review of Research Progress on ω -phase in Titanium Alloys, 11
240 (2022) 2022. <https://doi.org/10.37421/jme.2022.11.620>.
- 241 [12] S. Pilz, A. Hariharan, F. Günther, M. Zimmermann, A. Gebert, Influence of isothermal omega
242 precipitation aging on deformation mechanisms and mechanical properties of a β -type Ti-Nb alloy, *J*
243 *Alloys Compd* 930 (2023). <https://doi.org/10.1016/j.jallcom.2022.167309>.
- 244 [13] D. De Fontaine, Simple Models for the Omega Phase Transformation, *Metallurgical Transactions A* 19
245 (1988) 169–175.
- 246 [14] C. Talbot, N. Church, E. Hildyard, L. Connor, J. Miller, N. Jones, On the stability and formation of the α'
247 and ω phases in Ti-Nb alloys upon cooling, *Acta Mater* 262 (2024) 119409.
248 <https://doi.org/10.1016/j.actamat.2023.119409>.
- 249 [15] S.A. Mantri, D. Choudhuri, T. Alam, V. Ageh, F. Sun, F. Prima, R. Banerjee, Change in the deformation
250 mode resulting from beta-omega compositional partitioning in a Ti[β]-Mo alloy: Room versus
251 elevated temperature, *Scr Mater* 130 (2017) 69–73. <https://doi.org/10.1016/j.scriptamat.2016.11.013>.
- 252 [16] Y.L. Hao, S.J. Li, S.Y. Sun, C.Y. Zheng, R. Yang, Elastic deformation behaviour of Ti-24Nb-4Zr-7.9Sn for
253 biomedical applications, *Acta Biomater* 3 (2007) 277–286.
254 <https://doi.org/10.1016/j.actbio.2006.11.002>.
- 255 [17] F. Brumbauer, N.L. Okamoto, T. Ichitsubo, W. Sprengel, M. Luckabauer, Minor additions of Sn suppress
256 the omega phase formation in beta titanium alloys, *Acta Mater* 262 (2024).
257 <https://doi.org/10.1016/j.actamat.2023.119466>.
- 258 [18] S. Li, W.T. Lee, J.T. Yeom, J.G. Kim, J.S. Oh, T. Lee, Y. Liu, T.H. Nam, Towards bone-like elastic modulus
259 in Ti-Nb-Sn alloys with large recovery strain for biomedical applications, *J Alloys Compd* 925 (2022)
260 166724. <https://doi.org/10.1016/j.jallcom.2022.166724>.
- 261 [19] N.L. Okamoto, F. Brumbauer, M. Luckabauer, W. Sprengel, R. Abe, T. Ichitsubo, Why is neutral tin
262 addition necessary for biocompatible β -titanium alloys?—Synergistic effects of suppressing ω
263 transformations, *Acta Mater* 273 (2024). <https://doi.org/10.1016/j.actamat.2024.119968>.
- 264 [20] D.L. Moffat, D.C. Larbalestier, Competition Between Martensite and Omega in Quenched TiNb Alloys,
265 *Metallurgical Transactions A (Physical Metallurgy and Materials Science)* 19 A (1988) 1677–1686.
266 <https://link.springer.com/content/pdf/10.1007/BF02645135.pdf> (accessed September 19, 2019).
- 267 [21] L.W. Ma, H.S. Cheng, C.Y. Chung, B. Yuan, Effect of heat treatment time on microstructure and
268 mechanical properties of Ti-19Nb-9Zr (at%) shape memory alloy, *Materials Science and Engineering: A*
269 561 (2013) 427–433. <https://doi.org/10.1016/j.msea.2012.10.053>.
- 270 [22] E.W. Collings, *The physical metallurgy of titanium alloys*, American Society for Metals, 1984.
- 271 [23] S. Cai, J.E. Schaffer, Y. Ren, Deformation of a Ti-Nb alloy containing α -martensite and omega phases,
272 *Appl Phys Lett* 106 (2015). <https://doi.org/10.1063/1.4916960>.
- 273 [24] E.M. Hildyard, L.D. Connor, N.L. Church, T.E. Whitfield, N. Martin, D. Rugg, H.J. Stone, N.G. Jones, On
274 the role of internal stresses on the superelastic behaviour of Ti-24Nb (at.%), *Acta Mater* 237 (2022)
275 118161. <https://doi.org/10.1016/j.actamat.2022.118161>.
- 276 [25] D.C. Zhang, Y.F. Mao, M. Yan, J.J. Li, E.L. Su, Y.L. Li, S.W. Tan, J.G. Lin, Superelastic behavior of a B-type
277 titanium alloy, *J Mech Behav Biomed Mater* 20 (2013) 29–35.
278 <https://doi.org/10.1016/j.jmbbm.2013.01.015>.
- 279 [26] K. Endoh, M. Tahara, T. Inamura, H. Hosoda, Effect of Sn and Zr content on superelastic properties of
280 Ti-Mo-Sn-Zr biomedical alloys, *Materials Science and Engineering A* 704 (2017) 72–76.
281 <https://doi.org/10.1016/j.msea.2017.07.097>.

- 282 [27] E.M. Hildyard, L.D. Connor, L.R. Owen, D. Rugg, N. Martin, H.J. Stone, N.G. Jones, The influence of
283 microstructural condition on the phase transformations in Ti-24Nb (at.%), *Acta Mater* 199 (2020) 129–
284 140. <https://doi.org/10.1016/j.actamat.2020.08.004>.
- 285 [28] Y. Al-Zain, H.Y. Kim, T. Koyano, H. Hosoda, T.H. Nam, S. Miyazaki, Anomalous temperature dependence
286 of the superelastic behavior of Ti-Nb-Mo alloys, *Acta Mater* 59 (2011) 1464–1473.
287 <https://doi.org/10.1016/j.actamat.2010.11.008>.
- 288 [29] R. Natalia, B. Sergey, Entropy change in the B2→B19' martensitic transformation in TiNi alloy,
289 *Thermochim Acta* 602 (2015) 30–35. <https://doi.org/10.1016/j.tca.2015.01.004>.
- 290 [30] E.N.D. Grassi, G. Chagnon, H.M.R. de Oliveira, D. Favier, Anisotropy and Clausius-Clapeyron relation for
291 forward and reverse stress-induced martensitic transformations in polycrystalline NiTi thin walled
292 tubes, *Mechanics of Materials* 146 (2020) 103392. <https://doi.org/10.1016/j.mechmat.2020.103392>.
- 293 [31] H.Y. Kim, S. Hashimoto, J.I. Kim, T. Inamura, H. Hosoda, S. Miyazaki, Effect of Ta addition on shape
294 memory behavior of Ti-22Nb alloy, *Materials Science and Engineering A* 417 (2006) 120–128.
295 <https://doi.org/10.1016/j.msea.2005.10.065>.
- 296 [32] Y. Al-Zain, H.Y. Kim, H. Hosoda, T.H. Nam, S. Miyazaki, Shape memory properties of Ti-Nb-Mo
297 biomedical alloys, *Acta Mater* 58 (2010) 4212–4223. <https://doi.org/10.1016/j.actamat.2010.04.013>.
- 298 [33] M.F. Ijaz, H.Y. Kim, H. Hosoda, S. Miyazaki, Effect of Sn addition on stress hysteresis and superelastic
299 properties of a Ti-15Nb-3Mo alloy, *Scr Mater* 72–73 (2014) 29–32.
300 <https://doi.org/10.1016/j.scriptamat.2013.10.007>.
- 301 [34] N.L. Church, N.G. Jones, The influence of stress on subsequent superelastic behaviour in Ti2448 (Ti–
302 24Nb–4Zr–8Sn, wt%), *Materials Science and Engineering: A* 833 (2022) 142530.
303 <https://doi.org/10.1016/j.msea.2021.142530>.
- 304 [35] H.Y. Kim, Y. Ikehara, J.I. Kim, H. Hosoda, S. Miyazaki, Martensitic transformation, shape memory effect
305 and superelasticity of Ti-Nb binary alloys, *Acta Mater* 54 (2006) 2419–2429.
306 <https://doi.org/10.1016/j.actamat.2006.01.019>.
- 307 [36] H.Y. Kim, S. Miyazaki, Martensitic Transformation and Superelastic Properties of Ti-Nb Base Alloys,
308 *Mater Trans* 56 (2015) 625–634. <https://doi.org/10.2320/matertrans.M2014454>.
- 309 [37] H.Y. Kim, J. Fu, H. Tobe, J.I. Kim, S. Miyazaki, Crystal Structure, Transformation Strain, and Superelastic
310 Property of Ti–Nb–Zr and Ti–Nb–Ta Alloys, *Shape Memory and Superelasticity* 1 (2015) 107–116.
311 <https://doi.org/10.1007/s40830-015-0022-3>.
- 312 [38] F. Sun, J.Y. Zhang, P. Vermaut, D. Choudhuri, T. Alam, S.A. Mantri, P. Svec, T. Gloriant, P.J. Jacques, R.
313 Banerjee, F. Prima, Strengthening strategy for a ductile metastable β -titanium alloy using low-
314 temperature aging, *Mater Res Lett* 5 (2017) 547–553.
315 <https://doi.org/10.1080/21663831.2017.1350211>.
- 316 [39] H. Liu, M. Niinomi, M. Nakai, K. Cho, Athermal and deformation-induced ω -phase transformations in
317 biomedical beta-type alloy Ti-9Cr-0.2O, *Acta Mater* 106 (2016) 162–170.
318 <https://doi.org/10.1016/j.actamat.2016.01.008>.
- 319 [40] N.L. Church, C.E.P. Talbot, J.R. Miller, L.D. Connor, S. Michalik, N.G. Jones, Evidence of dislocation
320 dependent behaviour in superelastic Ti2448 (Ti-24Nb-4Zr-8Sn, wt%), *Acta Mater* 255 (2023).
321 <https://doi.org/10.1016/j.actamat.2023.119066>.
- 322 [41] ASTM International, ASTM E8/E8M Standard test methods for tension testing of metallic materials,
323 *Annual Book of ASTM Standards* (2013) 1–27. <https://doi.org/10.1520/E0008>.
- 324 [42] N.L. Church, C.E.P. Talbot, L.D. Connor, S. Michalik, N.G. Jones, The interdependence of the thermal
325 and mechanical cycling behaviour in Ti2448 (Ti-24Nb-4Zr-8Sn, wt%), *Materials Science and
326 Engineering: A* 899 (2024) 145791. <https://doi.org/10.1016/j.msea.2023.145791>.
- 327 [43] D. Preisler, Beta-Ti alloys for medical applications, Charles University, 2023.
- 328 [44] N.L. Church, A. Prasad, N.G. Jones, On the design of low modulus Ti–Nb–Au alloys for biomedical
329 applications, *J Mech Behav Biomed Mater* 157 (2024). <https://doi.org/10.1016/j.jmbbm.2024.106633>.

330

331